Experimental Determination of the Fusion-Barrier Distribution for the $^{154}Sm + ^{16}O$ Reaction

J. X. Wei, J. R. Leigh, D. J. Hinde, J. O. Newton, R. C. Lemmon, S. Elfstrom, and J. X. Chen
Department of Nuclear Physics, Research School of Physical Sciences, Australian National University, GPO Box 4, Canberra, Australian Capital Territory 2601, Australia

N. Rowley
Daresbury Laboratory (Science and Engineering Research Council), Daresbury, Warrington WA4 4AD, United Kingdom
(Received 12 June 1991)

The commonly held view that fusion excitation functions are featureless and do not provide a good test of models is challenged by high-precision measurements for the reaction $^{154}Sm + ^{16}O$. The data yield a well-defined distribution of barrier heights using a recently proposed, novel analysis technique. The measured distribution is that expected from the quadrupole deformation of ^{154}Sm and models using significantly different distributions cannot reproduce the measured excitation functions.

PACS numbers: 25.70.Jj

The enhancement of heavy-ion fusion at sub-barrier energies over that expected from penetration of a one-dimensional barrier is a widespread phenomenon [1] which has been qualitatively described in terms of coupling to inelastic and transfer channels [2]. This coupling results in a number of fusion barriers, distributed in energy, the lower ones being responsible for fusion at lower energies. Various forms of the barrier distribution have been assumed [3–5] in attempts to fit sub-barrier fusion cross sections. It has recently been suggested that the application of a novel analysis technique allows this distribution of barriers to be extracted directly from fusion data [6] without the imposition of arbitrary shapes and symmetries. Although not explicitly stated in Ref. [6], this challenges the commonly held view (see Ref. [7], for example) that excitation functions are smooth and featureless and can be reproduced by a wide range of models. The distribution of fusion barriers is revealed through subtle features of the excitation function which cannot then be reproduced by calculations incorporating significantly different barriers. Fusion excitation functions are therefore capable of revealing details of the fusion process which limit the range of applicable models. (It should be noted that this analysis depends on fusion resulting from barrier penetration. It may not be valid for fusion of very heavy nuclei, if effects such as neck formation are important.)

Existing excitation functions were not measured in sufficiently fine steps and with sufficiently small errors to define the shape of the distribution of barrier heights by the method of Ref. [6]. This was clearly illustrated in Ref. [6] where data [5] for the reactions $^{148,154}Sm + ^{16}O$ were analyzed. The experimental distributions for these two reactions, shown in Fig. 1, are indistinguishable, even though they are expected to differ considerably since ^{154}Sm has a large permanent quadrupole deformation while ^{148}Sm is "vibrational." The figure also demonstrates that the experimental distributions can equally well be described by a number of arbitrary functions. Thus it is clear that improved experimental data are required to determine the shape of the barrier height distribution by this method.

In order to check the validity of the proposed method [6], we have made high-precision measurements of evaporation residue cross sections at small and well-defined energy intervals, for the reaction $^{154}Sm + ^{16}O$. This reaction was chosen since the barrier distribution should result mainly from the target deformation and the extracted distribution can thus be compared with theoretical expectation.

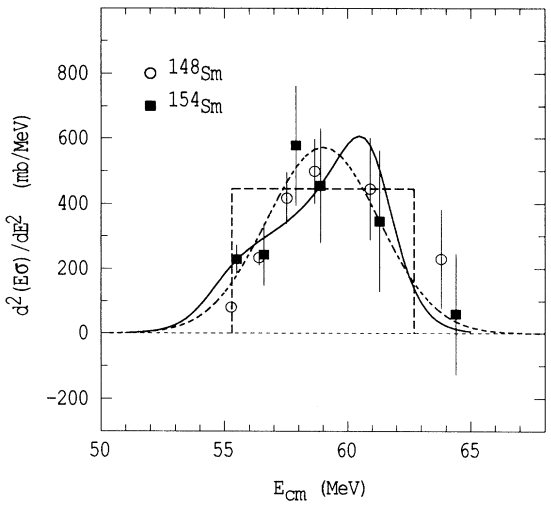

FIG. 1. Experimental barrier distributions $[d^2(E\sigma)/dE^2]$ for $^{148,154}Sm + ^{16}O$, adapted from Ref. [6]. The errors on the points are associated with a random error of 5% and are therefore smaller than those in Ref. [6] where systematic errors, which have little effect on the shape of the distribution, were also included. The curves, all reasonably consistent with the data, show two symmetric distributions (flat and Gaussian) and an asymmetric distribution, as expected from a target nucleus with a permanent quadrupole deformation.

Pulsed beams of ^{16}O ions (1 ns wide every 530 ns) in the energy range 58–110 MeV, from the Australian National University 14 UD pelletron, were used to bombard an isotopically enriched ^{154}Sm metal target, $\sim 40\ \mu g/cm^2$ in thickness on a carbon backing $\sim 20\ \mu g/cm^2$. Evaporation residues (ER) were measured at small angles ($\sim 1°$–$10°$) using a compact velocity filter [8] to deflect the intense elastic scattering away from a position-sensitive multiwire proportional counter (MWPC) located behind the filter and 600 mm from the target. The transmitted ER were identified by their time of flight (TOF) relative to the pulsed beam and their position and energy loss in the MWPC. The efficiency of the system for ER is consistent with 100%. At large angles ($\gtrsim 10°$) where elastic scattering is not overwhelming, ER were detected in a silicon surface-barrier detector and identified by their total energy and TOF.

Full angular distributions were measured at 65, 70, 74, 80, 90, 100, and 110 MeV. Typical examples are shown in Fig. 2. Total cross sections were extracted from these distributions by arbitrarily fitting with two Gaussian distributions; the narrower corresponds approximately to the combined effects of neutron and proton evaporation, and the wider to α emission, which is the most likely process to deflect ER to large angles. Typical fits are shown in Fig. 2. Fission has a probability of less than 0.1% at energies around the barrier so ER cross sections can be equated to fusion. The measured ER angular distributions show small, systematic deviations from the fitted Gaussians. To ensure that this did not affect the extracted cross sections, ER angular distributions for known fusion cross sections were calculated with the Monte Carlo code PACE2 [9], over the energy range 60–110 MeV. These distributions, which similarly deviate from the fitted shapes, were subjected to the same analysis and the extracted cross sections were consistently within 1% of the input values.

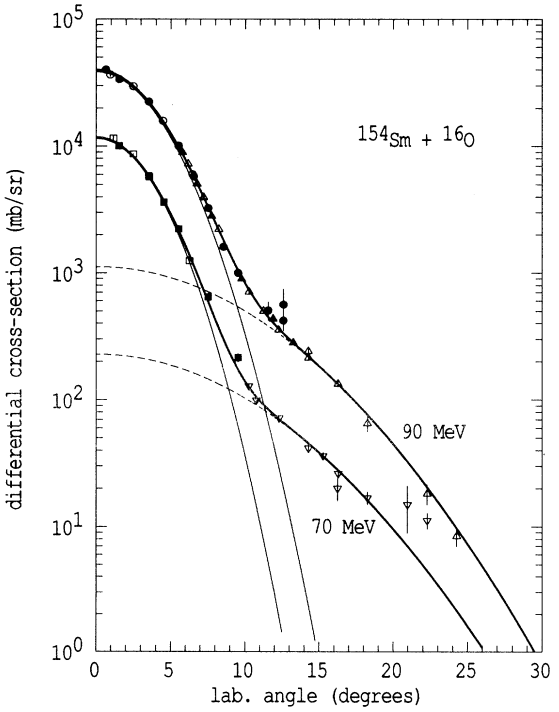

FIG. 2. Typical ER angular distributions for $^{154}Sm + ^{16}O$. The heavy lines are fits to the data, each comprising the sum of two Gaussian distributions (fine and dashed lines).

The shapes of the measured distributions vary slowly and smoothly with energy, enabling the ratio of the differential cross section, at a particular angle, to the total cross section to be accurately estimated at any energy. Thus the measurement of a differential cross section can be converted to a total fusion cross section. Since multiple scattering can affect the shape of the ER angular distribution, and hence the ratio of differential to total cross sections, the same target, oriented normal to the beam, was used for all measurements. Differential cross sections at $\pm 2°$ were measured over the energy range 58–74 MeV in 0.5-MeV intervals.

The magnetic field defining the lowest beam energy was derived after slowly recycling the current three times through the maximum and minimum values and then raising it to the required setting. Most of the other points were then obtained by successively raising the field, care being taken not to exceed the required value. Under these circumstances the 0.5-MeV interval is defined to a few keV. Several points were later repeated after further recycling of the magnet, in an attempt to avoid the problem of differential hysteresis. Monitor detectors, used for normalization purposes, also provided a check on the beam energy, though the energy defined by the magnet was accepted as the correct value. At one energy the cross section was lower than expected from neighboring points and the energy in the monitor was significantly lower than expected; this point was discarded. A paper describing details of the experiments and analysis is in preparation. The fusion cross sections thus obtained are shown in Fig. 3.

It has been shown [6] that the distribution of fusion barriers is related to the curvature $d^2(\sigma E)/dE^2$ which has been extracted from the data using cross sections σ_-, σ, and σ_+ at center-of-mass energies $E-\Delta E$, E, and $E+\Delta E$, respectively:

$$d^2(E\sigma)/dE^2 = \{(E-\Delta E)\sigma_- - 2E\sigma + (E+\Delta E)\sigma_+\}/\Delta E^2 . \quad (1)$$

The calculated values of $d^2(\sigma E)/dE^2$ are shown in Fig. 4 and represent the barrier distribution smoothed by the effects of quantum-mechanical tunneling. Figure 4(a) shows results for the subset of the data, mentioned above, for which the analyzing magnet was increased monotonically. Figure 4(b) shows all the data, including the repeated points.

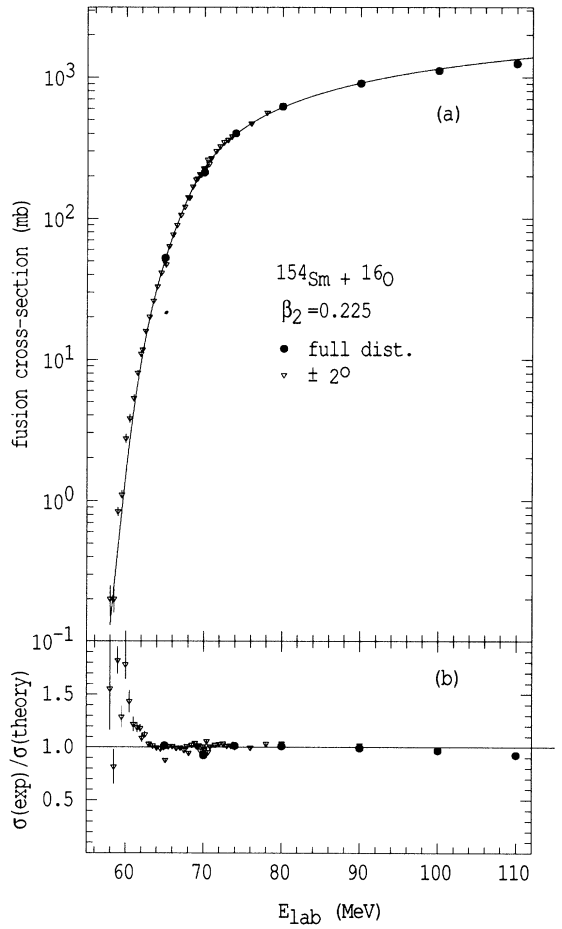

FIG. 3. (a) Fusion cross sections from full angular distributions and differential cross sections at $\pm 2°$. The curve is the result of a Wong model calculation using the classical barrier distribution of Fig. 4(a). (b) The ratio of experiment to calculation. The previous measurements of Ref. [5] are consistent with these data.

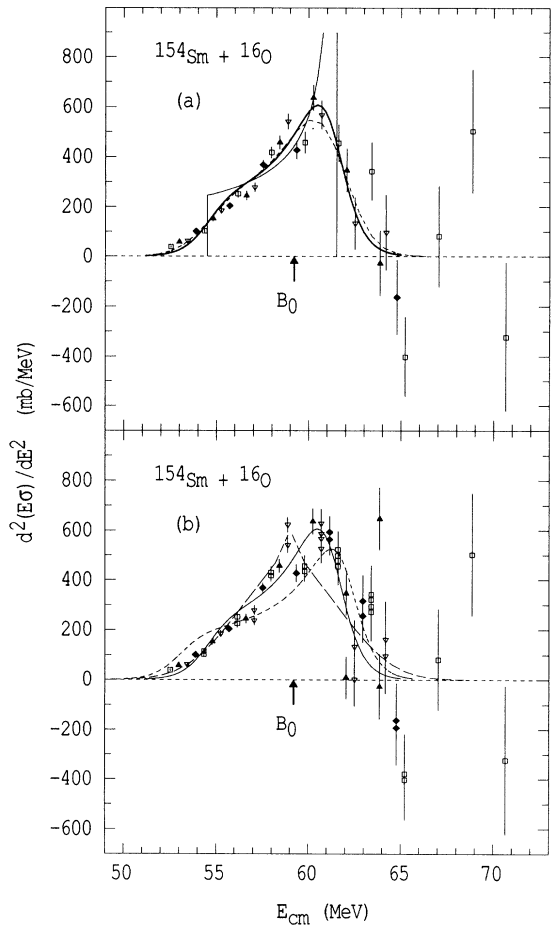

FIG. 4. Curvature $[d^2(\sigma E)/dE^2]$ from (a) data measured with monotonically increasing energy and (b) all data. Each point is evaluated using three cross sections; neighboring points with the *same* symbol have at least one of these cross sections in common and are therefore correlated. The curves in (a) are the classical barrier distribution for a target with a quadrupole deformation parameter $\beta=0.22$ (fine line), that smoothed by barrier penetration (heavy line), and the effect of analysis with $\Delta E=1.81$ MeV (dashed line). The curves in (b) correspond to the smoothed distribution (fine line) from (a), the distribution for $\beta=0.3$ (short-dashed line), and the distribution using the analysis of Ref. [4] (long-dashed line).

The statistical uncertainty δc associated with this curvature is given approximately by

$$\delta c \simeq (E/\Delta E^2)(\delta\sigma_-^2 + 4\delta\sigma^2 + \delta\sigma_+^2)^{1/2}, \quad (2)$$

where the $\delta\sigma$'s are random errors on the cross sections. To maintain a constant value of δc over the energy range of interest requires much higher statistical accuracy at higher energies. For instance, to achieve an error $\delta\sigma=1$ mb requires measurements of only 10% precision at $E\simeq 66$ MeV but 0.2% at 71 MeV. We ensured that statistical errors were $\lesssim 1$ mb for cross sections up to 100 mb and $\lesssim 1\%$ for higher values. Nonstatistical random errors were estimated from the reproducibility of the cross sections at seven different energies and by six measurements at one energy, after recycling the magnet, refocusing the beam, and resetting the velocity filter angles. The distribution of cross sections was generally consistent with a random error of 1%, even though statistical errors were significantly smaller. Thus the minimum random error was taken to be 1%. In one case, a difference in cross section of 7% was obtained and this was probably due to human error. This remeasured cross section results in the additional solid triangles at 62 and 64 meV in Fig. 4(b), displaced significantly from the other data, illustrating the care required in making these measurements.

The value of δc in Fig. 4 increases significantly with increasing energy as the magnitude of $\delta\sigma$ increases. It is

also evident from Eq. (2) that δc is inversely proportional to the square of the energy interval, ΔE^2. A value of 1.81 MeV (2 MeV in beam energy) gives acceptable values of δc and has only minor implications for the extracted distribution.

Systematic errors on the cross sections are expected to be small and in any case they are not important in defining the barrier distribution. For instance, a detection efficiency less than the expected 100% would simply result in a minor renormalization of the distribution without affecting its shape.

The distribution in Fig. 4 is evidently asymmetric, increasing slowly from 52 to 60 MeV, and then decreasing relatively quickly. The experimental distributions for ^{154}Sm in Fig. 1 are consistent with these data but the symmetric theoretical distributions are not.

It has been shown [10] that the barrier distribution from a coupled-channels approach, in which all members of the rotational band are included, is equivalent to the classical distribution expected from the different possible orientations of a target nucleus with a permanent quadrupole deformation. A classical distribution of barriers [6] is shown in Fig. 4(a); the effect on it of barrier penetration, together with the minor effect of using the 1.81-MeV step length, are also illustrated. These distributions were obtained with the spherical barrier $B_0=59.2$ MeV and $\pi R^2=3300$ mb, obtained from both the high-energy fusion data and the barrier curvature $\hbar\omega=4.2$ MeV from Ref. [6]. The target deformation parameter β was allowed to vary and the best fit was obtained using $\beta=0.22$, significantly lower than the value of $\beta\sim0.3$ from Coulomb excitation of ^{154}Sm [11] but consistent with that from previous fusion analyses [5]. The larger β value results in the much wider distribution shown in Fig. 4(b). The good fit with this form of barrier distribution provides experimental justification for the use of the Wong model [12] for this reaction. Fusion cross sections calculated with this model, for the classical distribution in Fig. 4(a), are compared with experiment in Fig. 3(b). The agreement is excellent for all but the lowest energies, where the smoothed theoretical barrier distribution is slightly lower than experiment [Fig. 4(a)] resulting in this deviation.

In summary, we have made precise measurements to determine the fusion excitation function for the reaction ^{154}Sm+^{16}O, at energies spanning the fusion barrier. For the first time, a well-defined fusion-barrier distribution has been extracted directly [6] from experimental data and this distribution clearly confirms that the deformation of ^{154}Sm is largely responsible for sub-barrier fusion enhancement. In contrast to the generally accepted view, these measurements demonstrate that fusion excitation functions carry considerable detail about the fusion process. However, this detail only becomes apparent when the random errors associated with the cross sections are about 1%, as in the present experiment.

[1] S. G. Steadman and M. J. Rhoades-Brown, Annu. Rev. Nucl. Sci. **36**, 649 (1988).
[2] C. S. Dasso *et al.*, Nucl. Phys. **A405**, 381 (1982); **A407**, 221 (1983); R. A. Broglia *et al.*, Phys. Rev. C **27**, 2433 (1983).
[3] L. C. Vaz and J. M. Alexander, Phys. Rev. C **10**, 464 (1974).
[4] P. Stelson *et al.*, Phys. Rev. C **41**, 1584 (1990).
[5] R. G. Stokstad *et al.*, Phys. Rev. Lett. **41**, 465 (1978); Phys. Rev. C **21**, 2427 (1980).
[6] N. Rowley *et al.*, Phys. Lett. B **254**, 25 (1991).
[7] A. H. Wuosmaa *et al.*, Phys. Lett. B **263**, 23 (1991).
[8] J. X. Wei *et al.*, Nucl. Instrum. Methods Phys. Res., Sect. A **306**, 557 (1991).
[9] A. Gavron, Phys. Rev. C **21**, 230 (1980).
[10] M. A. Nagarajan, A. B. Balantekin, and N. Takigawa, Phys. Rev. C **34**, 894 (1986).
[11] B. Harmatz, Nucl. Data Sheets **26**, 281 (1979).
[12] C. Y. Wong, Phys. Rev. Lett. **31**, 766 (1973).